

# Gesture Similarity Analysis on Event Data Using a Hybrid Guided Variational Auto Encoder

Kenneth Stewart  
University of California, Irvine  
Department of Computer Science  
kennetms@uci.edu

Lazar Supic  
Accenture Labs  
San Francisco, CA  
lazar.supic@accenture.com

Andreea Danielescu  
Accenture Labs  
San Francisco, CA  
andreea.danielescu@accenture.com

Timothy Shea  
Accenture Labs  
San Francisco, CA  
timothy.m.shea@accenture.com

Emre Neftci  
University of California, Irvine  
Department of Cognitive Science  
Department of Computer Science  
eneftci@uci.edu

## Abstract

*While commercial mid-air gesture recognition systems have existed for at least a decade, they have not become a widespread method of interacting with machines. This is primarily due to the fact that these systems require rigid, dramatic gestures to be performed for accurate recognition that can be fatiguing and unnatural. The global pandemic has seen a resurgence of interest in touchless interfaces, so new methods that allow for natural mid-air gestural interactions are even more important. To address the limitations of recognition systems, we propose a neuromorphic gesture analysis system which naturally declutters the background and analyzes gestures at high temporal resolution. Our novel model consists of an event-based guided Variational Autoencoder (VAE) which encodes event-based data sensed by a Dynamic Vision Sensor (DVS) into a latent space representation suitable to analyze and compute the similarity of mid-air gesture data. Our results show that the features learned by the VAE provides a similarity measure capable of clustering and pseudo labeling of new gestures. Furthermore, we argue that the resulting event-based encoder and pseudo-labeling system are suitable for implementation in neuromorphic hardware for online adaptation and learning of natural mid-air gestures.*

## 1. Introduction

Computers that can interact with users through touch and spoken language have become ubiquitous. However, people also communicate a great deal of information through body language and mid-air gestures, which are often closely coupled with speech [13]. This mode of interaction is beneficial in a variety of human computer interaction applications because it is natural, touchless, and efficient. For example, mid-air gestures can be used to interact with car infotainment systems, making interaction safer by eliminating the need for drivers to look at a touch interface instead of the road while driving [51] [32]. Mid-air gesture interaction can also be beneficial in high traffic public areas, reducing the need for touch based systems which can transmit pathogens from person to person. Additionally, interactive systems that leverage mid-air gestures are more accessible for people with hearing or speech impairments than other touchless alternatives, such as voice [5].

Despite numerous potential applications and recent progress in sensors capable of detecting mid-air gestures [29] [54] [23] [48], accurate recognition of mid-air gestures remains a challenge. Changing backgrounds and lighting conditions and wide variation in how users perform the same gesture are just a few of the reasons that accurate recognition in real-world environments is difficult. As a result, existing mid-air gesture recognition systems constrain users to performing predefined, rigid gestures and require large data sets to train. But this approach results in reduced accuracy in real-world settings because people have diffi-

culty reproducing or remembering rigid, precise movements [19]. A reliably accurate gesture recognition system needs to address these issues by being able to recognize natural gestures despite their wide ranging variability and changing backgrounds, and without relying on large datasets recorded in users' homes. Recording large vision datasets from users homes and sending the data to the cloud for model training would be both an invasion of privacy and a security risk for home owners and their families.

One way to address these issues is to adapt in real-time to user's individual gestures, by measuring the similarity of the incoming gesture to existing gesture classes. Neuromorphic Dynamic Vision Sensors (DVS) inspired by the biological retina are particularly well suited to this task [7], because they can capture temporal, pixel-wise intensity changes as a sparse stream of binary events, potentially enabling efficient learning at the edge [15]. This method of visual sensing has key advantages over traditional RGB cameras, such as faster response times, better temporal resolution, and invariance to static image features like lighting and background. However, effectively processing DVS event streams remains an open challenge. Unlike conventional frame-based cameras, events are asynchronous and spatially sparse, making it impossible to directly apply conventional vision algorithms [16, 15].

Spiking Neural Networks (SNNs) can efficiently process and learn from event-based data while taking advantage of temporal information [35]. SNN models are inspired by the biological cortex and can be used for hierarchical feature extraction from the precise timing of events through event-by-event processing [18]. Recent work demonstrated how SNNs can be trained end-to-end using gradient back-propagation in time and standard autodifferentiation tools, making the integration of SNNs possible as part of modern machine learning and deep learning methods [53, 6, 39].

Here, we take advantage of this capability by incorporating a convolutional SNN into a Variational Autoencoder (VAE) to encode spatio-temporal streams of events recorded by the DVS (figure 1). The goal of the VAE is to embed the streams of DVS events into a latent space which facilitates the evaluation of gesture similarity. In order to best use the underlying hardware, we implement a *hybrid* VAE algorithm to process the DVS data, where the encoder is SNN-based and the decoder is based on a conventional convolutional network. As some labelled data is included in the used dataset, we leverage a guided, supervised VAE to further disentangle the factors that account for gesture variation.

Our Hybrid Guided-VAE encodes the gesture data in a way that allows us to automatically measure and analyze the similarity of gestures, cluster similar gestures, and assign pseudo-labels to novel gestures. The key contributions of this work are:

1. End-to-end trainable event-based SNNs for processing neuromorphic sensor data event-by-event and embedding them in a latent space.

2. A Hybrid Guided-VAE that encodes event-based camera input and generates a latent space representation of the data that analyzes and calculates gesture similarity for clustering and pseudo-labeling.

The ability to measure gesture similarity from DVS data is a key feature to enable mid-air gesture recognition systems that are less rigid and more natural because they can adapt to each user.

## 2. Related Work

### 2.1. Measuring Gesture Similarity

Mid air gesture datasets are obtained through gesture elicitation studies. The goal of gesture elicitation studies is to collect user-defined gestures and then group similar gestures together to determine the gestural language for an application. One way the language is determined is by clustering gestures together based on a set of criteria [1] [47]. Examples of criteria used include but are not limited to which body part is used, body part trajectory, and body pose. For accuracy, humans typically observe which gestures are similar and cluster them. The goal of clustering the gestures and finding an agreement, or similarity measure is twofold. (1) the humans clustering the data provide labels for the data and explanations as to why they labeled a gesture a certain way based on the clustering criteria; and (2) the type of gesture most frequently used for a particular interaction can be identified.

There are several issues with current clustering methods. The clustering criteria used to evaluate which gestures are similar are chosen subjectively by researchers and therefore vary from study to study [9] [10] [40] [44]. Using subjective criteria contrasts with the goal of gesture elicitation studies, which is to find an objective consensus among the elicited gestures. The class labels given to the mid air gestures are also subjective and can vary across cultures. After clustering, a similarity score is calculated, with researchers continuously refining the appropriate similarity score to use [50] [46] [43] [45]. Additionally, because human labelers are needed, the process is tedious and expensive, which is why researchers are turning to crowd sourcing to reduce the time taken to cluster gesture data [1] [2].

To circumvent these issues, our work seeks to automate the process of computing gesture similarity from data for clustering. With recent advances in deep learning, the process of class labeling for image classification and object recognition tasks can be automated [4] or semi-automated [38]. Because mid air gesture data can be collected in the form of images or video, deep learning can be used for automatic gesture class labeling by learning a similarity measure between the gestures. However, it is still a challenging problem because salient image features may be missing in a scene or can be mistaken as part of the background. Additionally, mid air gestures are dynamic movements, so spatio-temporal information (*i.e.* video) processing is necessary for accurate recognition, which can be computation-

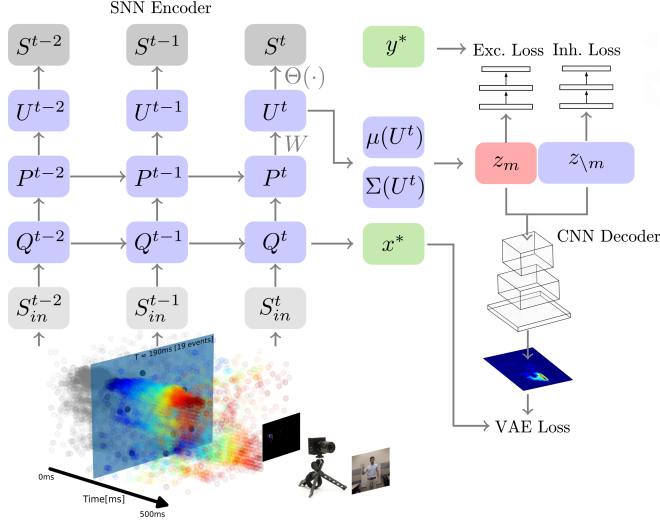


Figure 1: The Hybrid Guided-VAE architecture. Streams of gesture events recorded using a Dynamics Vision Sensor (DVS) are input into a Spiking Neural Network (SNN) that encodes the spatio-temporal features of the input data into a latent structure  $z$ .  $P$  and  $Q$  are pre-synaptic traces and  $U$  is the membrane potential of the spiking neuron. For clarity, only a single layer of the SNN is shown here and refractory states  $R$  are omitted. To help disentangle the latent space, a portion of the  $z$  equal to the number of target features  $y^*$  is input into a classifier that trains each latent variable to encode these features (Exc. Loss). The remaining  $z$ , noted  $\setminus m$  are input into a different classifier that adversarially trains the latent variables to not encode the target features so they encode for other features instead (Inh. Loss). The latent state  $z$  is decoded back into  $x^*$  using the conventional deconvolutional decoder layers.

ally expensive. Here, we automate the process of clustering mid air gestures for labeling using spatio-temporal event-based data streamed from a DVS. To automatically and objectively measure the similarity of gestures between and across classes for clustering and automatic labeling, we build a novel hybrid VAE model that can take advantage of the DVS’ temporal resolution and robustness while being end-to-end trainable using gradient descent on a variational objective.

## 2.2. Variational Autoencoders

VAEs are a type of generative model which deal with models of distributions  $p(x)$ , defined over data points  $x \in X$  [24]. A VAE commonly consists of two networks, 1) an encoder (*Enc*) that encodes the captured dependencies of a data sample  $x$  into a latent representation  $z$ ; and 2) a decoder (*Dec*) that decodes the latent representation back to the data space making a reconstruction  $\tilde{x}$ . Using Gaussian assumptions for the latent space :

$$Enc(x) = q(z|x) = N(z|\mu(x), \Sigma(x)) \quad (1)$$

$$\tilde{x} \approx Dec(z) = p(x|z), \quad (2)$$

where  $q$  is the encoding probability model into latent states  $z$  that are likely to produce  $x$ , and  $p$  is the decoding probability model conditioned  $z$ . The functions  $\mu(x)$  and  $\Sigma(x)$  are deterministic functions whose parameters can be trained through gradient-based optimization.

Using a variational approach, the VAE loss consists of the sum of two terms resulting from the variational lower bound:

$$\log p(x) \geq \underbrace{\mathbb{E}_{z \sim q} \log p(x|z)}_{\mathcal{L}_{ll}} - \underbrace{D_{KL}(q(z|x)||p(z))}_{\mathcal{L}_{prior}}. \quad (3)$$

The first term is the expected log likelihood of the reconstructed data computed using samples of the latent space,

and the second term acts as a prior, where  $D_{KL}$  is the Kullback-Leibler divergence. The VAE loss is thus formulated to maximize the variational lower bound by maximizing  $-\mathcal{L}_{prior}$  and  $\mathcal{L}_{ll}$ . VAE’s latent space captures salient information for representing the data  $X$ , and thus similarities in the data [26].

## 2.3. Disentangling Variational Autoencoders

VAEs do not necessarily disentangle all the factors of variation, which can make the latent space difficult to interpret and use. Several approaches have been developed to improve the disentangling of the latent representation, such as Beta VAE [20] and Total Correlation VAE [8]. Because existing gesture datasets are often already labeled by user, lighting condition and gesture class, it would be most advantageous to exploit these labels to guide the training of the VAE. For this reason, we employ a Guided-VAE, which has been developed specifically to disentangle the latent space representation of key features in a supervised fashion [12]. We describe here the supervised Guided-VAE algorithm, which is the basis of our hybrid model described in the next section.

To learn a disentangled representation, a supervised Guided-VAE trains latent variables to encode existing ground-truth labels while making the rest of the latent variables uncorrelated with that label. The supervised Guided-VAE model targets the generic generative modeling task by using an adversarial excitation and inhibition formulation. This is achieved by minimizing the discriminative loss for the desired latent variable while maximizing the minimal classification error for the rest of the latent variables. For  $N$  training data samples  $X = (x_1, \dots, x_N)$  and  $M$  features with ground-truth labels, let  $z = (z_1, \dots, z_m, \dots, z_M) \oplus z_{\setminus m}$  where the  $z_m$  define the “guided” latent variable capturing feature  $m$ , and  $z_{\setminus m}$  represents the rest of the latent variables. Let  $y_m(x_n)$  be a one-hot vector representing the ground-truth label for the  $m$ -th feature of sample  $x_n$ . For

each feature  $m$ , the excitation and inhibition losses are defined as follows:

$$\mathcal{L}_{Exc}(z, m) = \max_{c_m} \left( \sum_{n=1}^N \mathbb{E}_{q(z_m|x_n)} \log p_{c_m}(y = y_m(x_n)|z_m) \right) \quad (4)$$

$$\mathcal{L}_{Inh}(z, m) = \max_{k_m} \left( \sum_{n=1}^N \mathbb{E}_{q(z_{\setminus m}|x_n)} \log p_{k_m}(y = y_m(x_n)|z_{\setminus m}) \right) \quad (5)$$

where  $c_m$  is a classifier making a prediction on the  $m$ -th feature in the guided space and  $k_m$  is a classifier making a prediction over  $m$  in the unguided space  $z_{\setminus m}$ . By training these classifiers adversarially with the encoder part of the VAE, the encoder learns to disentangle the latent representation, with  $z_m$  representing the target features and  $z_{\setminus m}$  representing any features other than the target features.

### 3. Methods

#### 3.1. Dynamic Vision Sensors and Preprocessing

Dynamic Vision Sensors (DVS) are a type of event-based sensor that record event streams at a high temporal resolution and are compatible with SNNs [31]. Inspired by the human retina, DVS sensors detect events – or brightness changes – on a logarithmic scale with a user-tunable threshold, instead of RGB pixels like typical cameras. An event consists of the  $x, y$  location, timestamp  $t$ , and the polarity  $p \in [\text{OFF}, \text{ON}]$  representing direction of the intensity change. The DVS event stream is denoted  $S_{DVS,x,y,p}^t \in \{0, 1\}$ , where 1 indicates the presence of a spike at space-time coordinates  $(x, y, p, t)$ .

**Mapping DVS events to Network Inputs:** Recorded DVS events are streamed to a Hybrid Guided-VAE network implemented on a GPU (network dynamics described in the following section). At each time bin, the number of DVS events of each coordinate  $(x, y, p)$  are mapped onto two 2D channels of a convolutional layer, one for each polarity. With the selected time bin, most pixels take value zero, and very few take values larger than two. Note that time is *not* represented as a separate dimension in the convolutional layer, but through the dynamics of the SNN.

**Mapping DVS events to VAE Targets:** Time surfaces (TS) are widely used to preprocess event-based spatio-temporal features [25]. TS can be constructed by convolving an exponential decay kernel through time in the event stream as follows:

$$TS_{x,y,p}^t = \epsilon^t * S_{DVS,x,y,p}^t \text{ with } \epsilon^t = e^{-\frac{t}{\tau}} \quad (6)$$

where  $\tau$  is a time constant. Here, we convolve over the time length of the input gesture data stream  $S_{DVS,x,y,p}^t$ . This results in two 2D images, one for each polarity, that are used for the reconstruction loss.

#### 3.2. Hybrid Guided Variational Auto-Encoder

Gestures recorded using a DVS camera produce streams of events containing rich spatio-temporal patterns of the gesture. Event-based computer vision algorithms typically extract hand encoded statistics and use these in their models. While efficient, this approach discards important spatio-temporal features from the data [15]. Rather than manually selecting a feature set, we process the raw DVS events while preserving key spatio-temporal features using a spiking neural network (SNN) trained end-to-end in the Hybrid Guided-VAE architecture shown in figure 1.

A key advantage of the VAE is that the loss can be optimized using gradient backpropagation. To retain this advantage in our hybrid VAE, we must ensure that the encoder SNN is also trainable through gradient descent. Until recently, several challenges hindered this: the spiking nature of neurons’ nonlinearity makes it non-differentiable and the continuous-time dynamics raise a challenging temporal credit assignment problem. These challenges are solved by the surrogate gradients approach [35], which formulates the SNN as an equivalent binary RNN, and employs a smooth surrogate network for the purposes of computing the gradients.

Our Hybrid Guided-VAE uses a convolutional SNN to encode the spatio-temporal streams in the latent space, and a non-spiking convolutional decoder to reconstruct the TS of the data. Our choice of the event-based encoder is motivated by the fact that the SNN can bridge computational time scales, by extracting slow and relevant factors of variation in the gesture [49] from fast event streams recorded by the DVS.

Our choice of the conventional (non-spiking) decoder is motivated by the fact that (1) for gesture similarity estimation, we are mainly interested in the latent structure produced by the encoder, rather than the generative features of the network, (2) In a dedicated neuromorphic hardware implementation [21], only the encoder would be necessary to obtain this latent structure, and (3) SNN training is compute- and memory- intensive. Thus a conventional decoder enables us to dedicate more resources to the SNN encoder.

Hybrid VAEs that combine both spiking and ANN layers have been used before on DVS event data for predicting optical flow, and found that the hybrid architecture efficiently processes the sparse spatio-temporal event inputs while preserving the spatio-temporal nature of the events [27].

Our Hybrid Guided-VAE network architecture is shown in figure 1 and the architecture description is provided in Table 1. Descriptions of the excitatory and inhibitory networks are provided in the Supplementary Information (SI). The SNN encoder consists of four spiking convolutional layers followed by linear layers, and outputs a pair of vectors  $(\mu, \Sigma)$  for sampling the latent state  $z$ . According to the guided VAE, part of or all of latent state  $z$  is input into one of three connected networks, the excitation classifier, the adversarial inhibition classifier, or the decoder.

The target features for the excitatory network are given as one-hot encoded vectors of length  $M$ . The excitation classifier is jointly trained with the encoder to train the first  $M$  latent variables to only encode information relevant to the corresponding target feature. The inhibition classifier takes as input the remaining latent variables in the latent space,  $z_{\setminus m}$ , and are adversarially trained on two sets of targets. One set of targets are the same target features that the excitation classifier trains on. The other set of target features is a vector of length  $M$  but all of the values are set to 0.5 indicating that none of the values correspond to any target. The inhibition classifier is jointly trained with the encoder to train the remaining  $z_{\setminus m}$  latent variables to not encode any information relevant to target features forcing them to instead encode information for other features. The decoder is a transposed convolutional network that takes the full latent state  $z$  as input to construct the TS, denoted  $\tilde{x}$  in figure 1.

Table 1: Hybrid Guided-VAE Architecture.

Layer	Kernel	Output	Layer Type
input		$32 \times 32 \times 2$	DVS128
1	2a	$16 \times 16 \times 2$	SNN LIF Encoder
2	32c7p0s1	$16 \times 16 \times 32$	
3	1a	$16 \times 16 \times 32$	
4	64c7p0s1	$16 \times 16 \times 64$	
5	2a	$8 \times 8 \times 64$	
6	64c7p0s1	$8 \times 8 \times 64$	
7	1a	$8 \times 8 \times 64$	
8	128c7p0s1	$8 \times 8 \times 128$	
9	1a	$8 \times 8 \times 128$	
10	-	128	
11	-	100	$\mu(U^t)$ (ANN)
12	-	100	$\Sigma(U^t)$ (ANN)
13	-	128	ANN Decoder
14	128c4p0s2	$4 \times 4 \times 128$	Time Surface
15	64c4p1s2	$8 \times 8 \times 64$	
16	32c4p1s2	$16 \times 16 \times 32$	
output	2c4p1s2	$32 \times 32 \times 2$	

Notation: Ya represents  $Y \times Y$  sum pooling, XcYpZsS represents X convolution filters ( $Y \times Y$ ) with padding Z and stride S.

### 3.3. Encoder SNN Dynamics

To take full advantage of the event-based nature of the DVS input stream and its rich temporal features, the data is encoded using an SNN. SNNs can be formulated as a type of recurrent neural network with binary activation functions (Figure 1) [35]. With this formulation, SNN training can be carried out using standard tools of autodifferentiation. In particular, to best match the dynamics of existing digital neuromorphic hardware implementing SNNs [11, 14], our neuron model consists of a discretized Leaky Integrate and

Fire (LIF) neuron model with time step  $\Delta t$  [22]:

$$\begin{aligned}
 U_i^t &= \sum_j W_{ij} P_j^t - U_{th} R_i^t + b_i, \\
 P_j^{t+\Delta t} &= \alpha P_j^t + (1 - \alpha) Q_j^t, \\
 Q_j^{t+\Delta t} &= \beta Q_j^t + (1 - \beta) S_{in,j}^t, \\
 S_i^t &= \Theta(U_i^t),
 \end{aligned}
 \tag{7}$$

where the constants  $\alpha = \exp(-\frac{\Delta t}{\tau_{mem}})$  and  $\beta = \exp(-\frac{\Delta t}{\tau_{syn}})$  reflect the decay dynamics of the membrane potential and the synaptic state during a  $\Delta t$  timestep, where  $\tau_{mem}$  and  $\tau_{syn}$  are membrane and synaptic time constants, respectively. The time step in our experiments was fixed to  $\Delta t = 1$ ms.  $R_i$  here implements the reset and refractory period of the neuron, and states  $P_i, Q_i$  are pre-synaptic traces that capture the leaky dynamics of the membrane potential and the synaptic currents.  $S_i^t = \Theta(U_i^t)$  represents the spiking non-linearity, computed using the unit step function, where  $\Theta(U_i) = 0$  if  $U_i < U_{th}$ , otherwise 1. We distinguish here the input spike train  $S_{in}^t$  from the output spike train  $S^t$ . Following the surrogate gradient approach [35], for the purposes of computing the gradient, the derivative of  $\Theta$  is replaced with the derivative of the fast sigmoid function [52]. Note that equation (7) is equivalent to a discrete-time version of the spike response model with linear filters [17]. Similar networks were used for classification tasks on the DVSGesture dataset, leading to state-of-the-art accuracy on that task [22, 39]. In the SI, we show how these equations can be obtained via discretization of the common LIF neuron.

The SNN follows a convolutional architecture, as described in Table 1, encoding the input sequence  $S_{in}^t$  into a membrane potential variable  $U^t$  in the final layer. The network computes  $\mu(U^t)$  and  $\Sigma(U^t)$  as in a conventional VAE, but using the final membrane potential state  $U^t$ . Thanks to the chosen neural dynamics, the TS can be naturally computed by our network. In fact, using an appropriate choice of  $\tau = \tau_{syn}$  for computing the TS, it becomes exactly equivalent to the pre-synaptic trace  $Q^t$  of our network (See SI). Hence, our choice of input and target indeed corresponds to an autoencoder in the space of pre-synaptic traces  $Q^t$ .

### 3.4. Datasets

Our results are shown for datasets that were collected using DVS sensors [28, 37], the Neuromorphic MNIST (NMNIST) and IBM DvsGesture datasets. NMNIST consists of  $32 \times 32$ , 300ms long event data streams of MNIST images recorded with a DVS [36]. The dataset contains 60,000 training event streams and 10,000 test event streams. The IBM DvsGesture dataset [3] consists of recordings of 29 different individuals performing 10 different actions such as clapping and an unspecified gesture that serves as a “catch-all” for gestures that do not fit into the other 10 ac-

tions for a total of 11 classes [3]. The actions are recorded under four different lighting conditions, so each gesture is also labeled with the associated lighting condition under which it was performed. Samples from the first 23 subjects were used for training and the last 6 subjects were used for testing. The training set contains 1078 samples and the test set contains 264 samples. Each sample consists of about 6 seconds of the gesture performed. In our work we scale each sequence to 32x32 and only use a randomly sampled 200ms sequence of each sample to match real time learning conditions of the gesture data. For both datasets, to reduce memory requirements, the gradients were truncated to 100 time steps (*i.e.* 100ms worth of data). The input events are summed in  $\Delta t = 1\text{ms}$  time bins and then fed to the network. We use the IBM DvsGesture dataset because it is currently the only full body gesture dataset available that uses recordings from an event based camera. The task is to learn a latent space encoding that can be used to both reconstruct the digits or gestures and to learn the similarities in the data so that similar data points can be clustered and pseudo labels assigned.

Our choice for the event-based datasets above is further motivated by the nature of neuromorphic computing: the applications of neuromorphic sensors and computing are justified primarily when applied to event-based data, and particularly when features are embedded in the spatio-temporal features of the data. For this reason, we cannot meaningfully test on standard image datasets such as CIFAR and ImageNet.

## 4. Results

To analyze the similarity between data samples in the latent space we examine the accuracy of the excitation classifier in correctly identifying a gesture, T-SNE projections of the different parts of the latent space, latent space traversals, and the effect of using different guiding variables, namely lighting conditions. Finally, we observe the quality of the embeddings based on our own DVS recordings of novel gestures.

**Accuracy and Reconstruction:** The excitation classifier trained on the latent space of the hybrid VAE using the MNIST dataset achieves a training accuracy of approximately 99% and a test accuracy of approximately 99%, indicating that the SNN encoder is learning a latent representation that is able to disentangle along the target features. The excitation classifier results on the DvsGesture dataset without the eleventh “other” class achieves a training accuracy of approximately 99% and test accuracy of approximately 87%, indicating the SNN encoder is learning a disentangled latent representation of features unique to each gesture class but is having some difficulty distinguishing between certain gestures that are very similar.

In Figure 2, a sample gesture from each of the gesture classes is visualized as a time surface. Color in the samples corresponds to the TS value of the events at the end of the sequence. Note that the TS leaves a significant amount

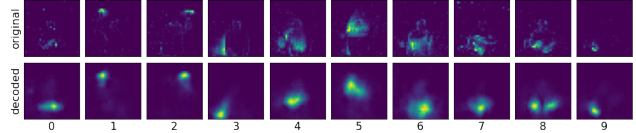


Figure 2: Original (top) and reconstructed (bottom) time-surfaces for a sample gesture from each class. The reconstructions reflect the location of each gesture but with some smoothing of the detail.

of fine detail intact. In contrast, encoding and then decoding the samples results in a reconstruction that preserves the general structure of the gesture but smooths out some of the detail. Note that the fidelity of the autoencoder is less important than the capacity of the model to disentangle the gesture classes. Furthermore, disentangling autoencoders are known to provide lower quality reconstructions compared to the vanilla VAE [8].

**Latent Space Projections:** We use T-SNE to examine the capacity of the network to disentangle key features of gestures in the latent space. T-SNE embeds both the local and global topology of the latent space into a low-dimensional visualization [34], allowing us to visualize clustering and separation between gesture classes and lighting conditions.

Figure 3 shows a T-SNE scatter plot of the guided portion of the latent space trained on the MNIST dataset. As expected, each trained digit class is separated into its own cluster, demonstrating the ability of the Hybrid Guided-VAE’s to disentangle the noisy input domain in its latent space representations.

Figure 4 shows a T-SNE plot of the guided portion of the latent space trained on the DvsGesture dataset. The latent space is clustered by the gesture that the excitation classifier targeted for each of the  $z_m$ , with some overlap between very similar gestures such as left arm clockwise versus left arm counterclockwise. The bottom of the figure shows samples from the “other” class in the Dvs Gesture dataset in relation to the T-SNE projection of the guided latent space. The embedded positions of these gestures show which gesture classes they are most similar to. For example, gestures with certain salient features, such as a salient left hand, are placed with the cluster of the gesture class that has the same salient feature, such as the left hand wave class. Thus, the latent states obtained for these gestures can provide the basis for pseudolabeling of new gestures by measuring the similarity between unclassified samples and existing gesture classes in the latent space.

**DvsGesture Latent Traversals:** We use latent traversals to reveal additional structure within the latent space. Traversals of the guided dimensions of the latent space are shown in Figure 5. Each image shown in the figure is a time-surface based on a position in the latent space computed using off polarity events. From left to right, the images represent a traversal from the minimum to the maximum value of a given guided dimension.

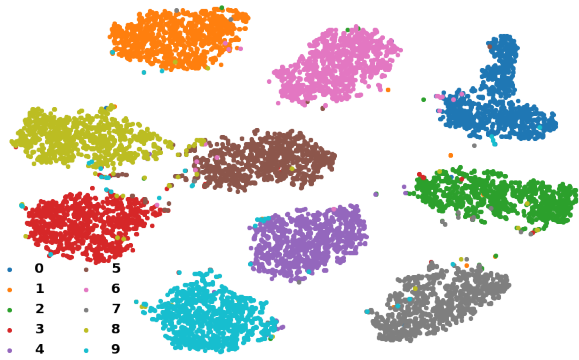


Figure 3: A T-SNE plot of the  $z_m$  portion of the latent space of the encoded MNIST dataset. The digits are accurately clustered.

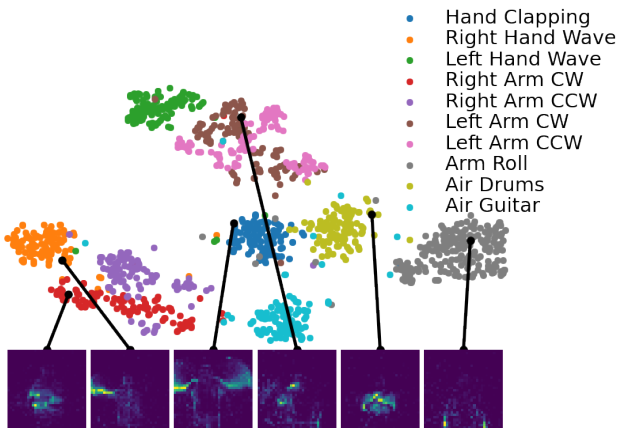


Figure 4: A T-SNE plot of the  $z_m$  portion of the latent space of the encoded Dvs Gesture dataset. The gestures are clearly clustered by class, indicating the latent space disentangled each of the gestures. Gestures with similar motion, such as air drums and arm roll, are also globally more similar than gestures qualitatively different motion, such as right hand wave and arm roll. Six unclassified gestures (labeled “other” in the dataset) are shown below as time-surfaces connected to the respective embedded positions in the latent space. Each of the unclassified gestures are embedded near gesture classes which exhibit similar motion.

Figure 6 shows different dimensions of the latent space to demonstrate that the Hybrid Guided-VAE has learned a disentangled feature representation of the DVSGestures. The latent space variables are fixed except for the second and third  $z_m$  variables that represent a right hand wave and a left hand wave respectively. The top panel of Figure 6 shows reconstructions when the right hand wave  $z_m$  is high (left) and the rest of the  $z_m$  are low while the right-most image has the left hand wave  $z_m$  high and the remaining  $z_m$  are low. The images in-between show the incremental transition between these values. Figure 6 (bottom) shows the effect of the  $z_m$  latent variables on a right hand gesture. As

the values of the  $z_m$  variables change the gesture remains the same, however the position, orientation, and saliency of the hand and arm changes suggesting that the Hybrid Guided-VAE represents the variability within the gesture type.

**Guiding on Light Conditions:** A key feature of the guided VAE is to incorporate alternative features not directly related to the gesture class to disentangle the factors of variation in the data. To demonstrate this, in a separate experiment, we trained on the lighting condition provided in the DVSGesture dataset instead of the gesture class. The T-SNE projection of the  $z_m$  latent space is shown in Figure 7a. The model clusters the lighting conditions with some overlap between LED lighting and the other lighting conditions. This is likely due to the fact that the lighting conditions under which the gestures are performed are combinations of the labeled lighting conditions, with the label given to the most prominent lighting condition used [3]. Figure 7b shows a T-SNE projection of the  $z_m$  latent space but is labeled by gesture class instead of lighting. The projection shows clustering of the gesture classes, particularly the classes that share similarities such as right hand wave, right arm clockwise, and right arm counterclockwise. This shows evidence that while the  $z_m$  space is learning features key to the lighting, the  $z_m$  is learning features key to the gesture class instead.

**Embeddings of Self-Recorded Gestures:** So far, all the gesture data used for the VAE originated from the DVSGestures dataset, which featured well controlled lighting and positioning conditions. Here, we evaluate how such a VAE would perform under less controlled conditions. We recorded two new classes of gestures not present in the DVSGesture dataset on a different DVS sensors (the DAVIS 240C sensor [7]) and input to the Hybrid Guided-VAE. We recorded three instances of each class, right swipe down and left swipe down for approximately 3s by the same subject under the same lighting condition. Figure 8 shows the gesture time surfaces and their associated T-SNE embeddings in the  $z_m$  portion of the latent space. All of the right swipe down gestures were evaluated by our VAE as being most similar to right hand wave gestures, which is seen in their position in the T-SNE of the latent space. The excitation classifier labeled each of the right swipe down gestures as right hand waves. All of the left swipe down gestures were evaluated by our VAE as being most similar to left hand wave gestures, which is seen in their position in the T-SNE of the latent space. The excitation classifier labeled each of the left swipe down gestures as left hand waves. The results shown in Figure 8 demonstrate that our Hybrid Guided-VAE is able to appropriately process, cluster, and label novel gestures.

## 5. Discussion and Future Work

We presented a novel Hybrid Guided-VAE algorithm to process DVS sensor data that uses an SNN encoder to encode spike events into a latent representation that is jointly

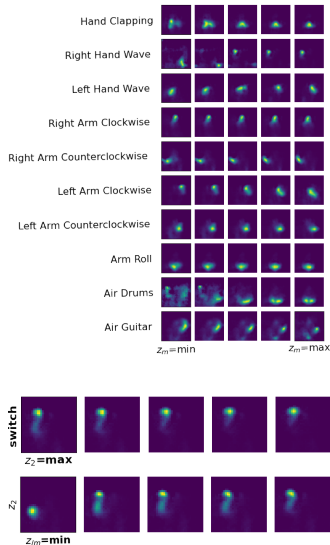


Figure 5: Reconstructions of latent traversals across each guided latent dimension. Each  $z_m$  represents a gesture class.

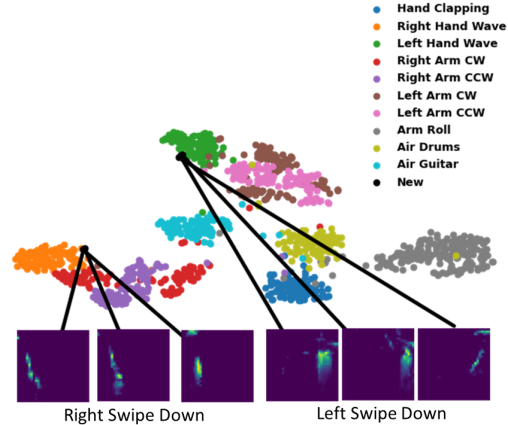


Figure 8: Projections of the  $z_m$  portion of the latent space of encoded new gestures we recorded using a different DVS, and not part of the DVSGesture dataset.

Figure 6: **Examination of the disentangled latent space:** (Top) Beginning with the right hand wave latent variable maximized and the left hand wave variable minimized, traverse along the latent space by gradually decreasing the right hand wave latent variable and increasing the left hand wave latent variable. (Bottom) Latent traversal along the latent space of non target  $z_{\setminus m}$  latent variables.

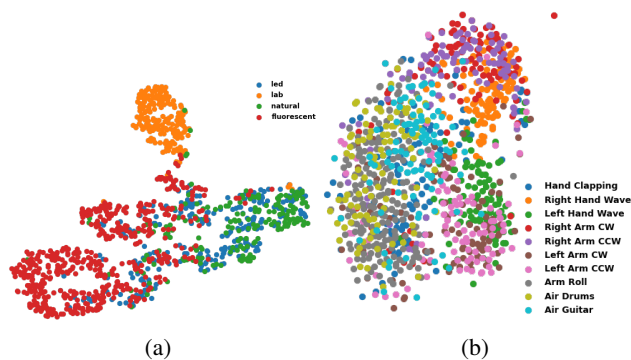


Figure 7: (a) A T-SNE plot of the guided portion of  $z$  using lighting condition labels. (b) A T-SNE plot of the corresponding unguided variables guided but labeled with gesture classes. The unguided latent space is encoding features relevant to the gesture being performed, such as which parts of the bodies perform the gesture.

trained by two classifiers to disentangle and encode target features. The goal of the algorithm is to understand the similarity of data, such as gestures, streamed to the network to existing classes in order to apply pseudo labels.

Our results demonstrate that the Hybrid Guided-VAE is able to disentangle the latent space of encoded event data based on the features the classifier is guided on. Therefore the VAE is learning a similarity measure for the event data that can be used to cluster the disentangled latent space by the guided target features for gesture similarity measurements. We also showed that with a SNN encoder and latent

space classifier, the model can be used to determine pseudo labels for incoming unlabeled data based on its similarity to classes of previously seen data which can be used for self-supervised or semi-supervised learning.

Thanks to the sparse nature of event-based data and processing, our SNN encoding implementation is interesting for applications at the edge, such as in a home or on a mobile device, where computing power is limited and privacy is paramount. While our GPU-based solution does not run in real-time and does not leverage spatio-temporal sparsity, dedicated neuromorphic hardware can leverage this sparsity for real-time, compact, ultra-low power processing [11, 30, 33]. Looking forward to such an implementation, our SNN model was chosen to be compatible with a previously demonstrated method of few-shot learning at low-power on the Intel Loihi Neuromorphic Research Chip [41].

One limitation of this work is the lack of benchmarking or a dataset that allows for comparison between different similarity measures. Additionally, there is no publicly available data in event-based, frame-based, and pose-point datasets using the same data samples that allows for comparison to other methods to such as [45]’s dissimilarity measurement using body pose data.

## 6. Conclusion

This work sets the foundation for a real-time neuromorphic implementation which can induce a gesture optimized latent state corresponding to novel gestures streamed from an event-based camera. The generated signals can be used to perform online self-supervised learning to update a recognition model on the fly [42], enabling applications such as life long learning for full body gesture interaction.

## References

[1] Abdullah X. Ali, Meredith Ringel Morris, and Jacob O. Wobbrock. Crowdsourcing similarity judgments for agree-



- ment analysis in end-user elicitation studies. *UIST '18*, page 177–188, New York, NY, USA, 2018. Association for Computing Machinery.
- [2] Abdullah X. Ali, Meredith Ringel Morris, and Jacob O. Wobbrock. Crowdlicit: A system for conducting distributed end-user elicitation and identification studies. In *Proceedings of the 2019 CHI Conference on Human Factors in Computing Systems*, CHI '19, page 1–12, New York, NY, USA, 2019. Association for Computing Machinery.
  - [3] Arnon Amir, Brian Taba, David Berg, Timothy Melano, Jeffrey McKinstry, Carmelo Di Nolfo, Tapan Nayak, Alexander Andreopoulos, Guillaume Garreau, Marcela Mendoza, et al. A low power, fully event-based gesture recognition system. In *Proceedings of the IEEE Conference on Computer Vision and Pattern Recognition*, pages 7243–7252, 2017.
  - [4] M Bah, Adel Hafiane, and Raphael Canals. Deep learning with unsupervised data labeling for weed detection in line crops in uav images. *Remote Sensing*, 10(11):1690, Oct 2018.
  - [5] Fabio Ballati, Fulvio Corno, and Luigi De Russis. Assessing virtual assistant capabilities with italian dysarthric speech. In *Proceedings of the 20th International ACM SIGACCESS Conference on Computers and Accessibility*, ASSETS '18, page 93–101, New York, NY, USA, 2018. Association for Computing Machinery.
  - [6] Guillaume Bellec, Franz Scherr, Elias Hajek, Darjan Salaj, Robert Legenstein, and Wolfgang Maass. Biologically inspired alternatives to backpropagation through time for learning in recurrent neural nets. *arXiv preprint arXiv:1901.09049*, 2019.
  - [7] Christian Brandli, Raphael Berner, Minhao Yang, Shih-Chii Liu, and Tobi Delbruck. A  $240 \times 180 \times 130$  db  $3 \mu\text{s}$  latency global shutter spatiotemporal vision sensor. *IEEE Journal of Solid-State Circuits*, 49(10):2333–2341, 2014.
  - [8] Ricky T. Q. Chen, Xuechen Li, Roger B Grosse, and David K Duvenaud. Isolating sources of disentanglement in variational autoencoders. In S. Bengio, H. Wallach, H. Larochelle, K. Grauman, N. Cesa-Bianchi, and R. Garnett, editors, *Advances in Neural Information Processing Systems*, volume 31. Curran Associates, Inc., 2018.
  - [9] Sabrina Connell, Pei-Yi Kuo, Liu Liu, and Anne Marie Piper. A wizard-of-oz elicitation study examining child-defined gestures with a whole-body interface. In *Proceedings of the 12th International Conference on Interaction Design and Children*, IDC '13, page 277–280, New York, NY, USA, 2013. Association for Computing Machinery.
  - [10] Sabrina Connell, Pei-Yi Kuo, Liu Liu, and Anne Marie Piper. A wizard-of-oz elicitation study examining child-defined gestures with a whole-body interface. In *Proceedings of the 12th International Conference on Interaction Design and Children*, IDC '13, page 277–280, New York, NY, USA, 2013. Association for Computing Machinery.
  - [11] M. Davies, N. Srinivasa, T. H. Lin, G. China, P. Joshi, A. Lines, A. Wild, and H. Wang. Loihi: A neuromorphic manycore processor with on-chip learning. *IEEE Micro*, PP(99):1–1, 2018.
  - [12] Zheng Ding, Yifan Xu, Weijian Xu, Gaurav Parmar, Yang Yang, Max Welling, and Zhuowen Tu. Guided variational autoencoder for disentanglement learning. In *Proceedings of the IEEE/CVF Conference on Computer Vision and Pattern Recognition (CVPR)*, June 2020.
  - [13] Marlen Fröhlich, Christine Sievers, Simon W. Townsend, Thibaud Gruber, and Carel P. van Schaik. Multimodal communication and language origins: integrating gestures and vocalizations. *Biological Reviews*, 94(5):1809–1829, 2019.
  - [14] Steve B Furber, Francesco Galluppi, Sally Temple, Luis Plana, et al. The spinnaker project. *Proceedings of the IEEE*, 102(5):652–665, 2014.
  - [15] Guillermo Gallego, Tobi Delbruck, Garrick Orchard, Chiara Bartolozzi, Brian Taba, Andrea Censi, Stefan Leutenegger, Andrew Davison, Jörg Conradt, Kostas Daniilidis, et al. Event-based vision: A survey. *arXiv preprint arXiv:1904.08405*, 2019.
  - [16] G. Gallego, T. Delbruck, G. M. Orchard, C. Bartolozzi, B. Taba, A. Censi, S. Leutenegger, A. Davison, J. Conradt, K. Daniilidis, and D. Scaramuzza. Event-based vision: A survey. *IEEE Transactions on Pattern Analysis and Machine Intelligence*, pages 1–1, 2020.
  - [17] W. Gerstner and W. Kistler. *Spiking Neuron Models. Single Neurons, Populations, Plasticity*. Cambridge University Press, 2002.
  - [18] Wulfram Gerstner, Werner M Kistler, Richard Naud, and Liam Paninski. *Neuronal dynamics: From single neurons to networks and models of cognition*. Cambridge University Press, 2014.
  - [19] Noorkholis Luthfil Hakim, Timothy K. Shih, Sandeli Priyanwada Kasthuri Arachchi, Wisnu Aditya, Yi-Cheng Chen, and Chih-Yang Lin. Dynamic hand gesture recognition using 3dcnn and lstm with fsm context-aware model. *Sensors (Basel, Switzerland)*, 19(24):5429, Dec 2019. 31835404[pmid].
  - [20] I. Higgins, Loïc Matthey, A. Pal, C. Burgess, Xavier Glorot, M. Botvinick, S. Mohamed, and Alexander Lerchner. beta-vae: Learning basic visual concepts with a constrained variational framework. In *ICLR*, 2017.
  - [21] G. Indiveri, B. Linares-Barranco, T.J. Hamilton, A. van Schaik, R. Etienne-Cummings, T. Delbruck, S.-C. Liu, P. Dudek, P. Häfliger, S. Renaud, J. Schemmel, G. Cauwenberghs, J. Arthur, K. Hynna, F. Folowosele, S. Saighi, T. Serrano-Gotarredona, J. Wijekoon, Y. Wang, and K. Boahen. Neuromorphic silicon neuron circuits. *Frontiers in Neuroscience*, 5:1–23, 2011.
  - [22] Jacques Kaiser, Hesham Mostafa, and Emre Neftci. Synaptic plasticity dynamics for deep continuous local learning (decolle). *Frontiers in Neuroscience*, 14:424, 2020.
  - [23] Leonid Keselman, John Iselin Woodfill, Anders Grunnet-Jepsen, and Achintya Bhowmik. Intel realsense stereoscopic depth cameras. In *Proceedings of the IEEE Conference on Computer Vision and Pattern Recognition (CVPR) Workshops*, July 2017.
  - [24] Diederik P Kingma and Max Welling. Auto-encoding variational bayes. *arXiv preprint arXiv:1312.6114*, 2013.
  - [25] X. Lagorce, G. Orchard, F. Galluppi, B. E. Shi, and R. B. Benosman. Hots: A hierarchy of event-based time-surfaces for pattern recognition. *IEEE Transactions on Pattern Analysis and Machine Intelligence*, 39(7):1346–1359, 2017.
  - [26] Anders Boesen Lindbo Larsen, Søren Kaae Sønderby, Hugo Larochelle, and Ole Winther. Autoencoding beyond pixels using a learned similarity metric. volume 48 of *Proceedings of Machine Learning Research*, pages 1558–1566, New York, New York, USA, 20–22 Jun 2016. PMLR.

- [27] Chankyu Lee, Adarsh Kumar Kosta, Alex Zihao Zhu, Kenneth Chaney, Kostas Daniilidis, and Kaushik Roy. Spike-flownet: Event-based optical flow estimation with energy-efficient hybrid neural networks, 2020.
- [28] P. Lichtsteiner, C. Posch, and T. Delbruck. A 128x128 120 dB 15 us latency asynchronous temporal contrast vision sensor. *Solid-State Circuits, IEEE Journal of*, 43(2):566–576, Feb. 2008.
- [29] P. Lichtsteiner, C. Posch, and T. Delbruck. An 128x128 120dB 15 $\mu$ s-latency temporal contrast vision sensor. *IEEE J. Solid State Circuits*, 43(2):566–576, 2008.
- [30] Qian Liu, Ole Richter, Carsten Nielsen, Sadique Sheik, Giacomo Indiveri, and Ning Qiao. Live demonstration: face recognition on an ultra-low power event-driven convolutional neural network asic. In *Proceedings of the IEEE/CVF Conference on Computer Vision and Pattern Recognition Workshops*, pages 0–0, 2019.
- [31] S.-C. Liu and T. Delbruck. Neuromorphic sensory systems. *Current Opinion in Neurobiology*, 20(3):288–295, 2010.
- [32] Keenan R. May, Thomas M. Gable, and Bruce N. Walker. Designing an in-vehicle air gesture set using elicitation methods. In *Proceedings of the 9th International Conference on Automotive User Interfaces and Interactive Vehicular Applications*, AutomotiveUI '17, page 74–83, New York, NY, USA, 2017. Association for Computing Machinery.
- [33] Christian Mayr, Sebastian Hoepfner, and Steve Furber. Spinnaker 2: A 10 million core processor system for brain simulation and machine learning. *arXiv preprint arXiv:1911.02385*, 2019.
- [34] Sudipto Mukherjee, Himanshu Asnani, Eugene Lin, and Sreeram Kannan. Clustergan: Latent space clustering in generative adversarial networks. *Proceedings of the AAAI Conference on Artificial Intelligence*, 33(01):4610–4617, Jul. 2019.
- [35] E. O. Neftci, H. Mostafa, and F. Zenke. Surrogate gradient learning in spiking neural networks: Bringing the power of gradient-based optimization to spiking neural networks. *IEEE Signal Processing Magazine*, 36(6):51–63, Nov 2019.
- [36] Garrick Orchard, Ajinkya Jayawant, Gregory K. Cohen, and Nitish Thakor. Converting static image datasets to spiking neuromorphic datasets using saccades. *Frontiers in Neuroscience*, 9, nov 2015.
- [37] C. Posch, D. Matolin, and R. Wohlgenannt. A qvga 143 db dynamic range frame-free pwm image sensor with lossless pixel-level video compression and time-domain cds. *Solid-State Circuits, IEEE Journal of*, 46(1):259–275, jan. 2011.
- [38] Krittaphat Pugdeethosapol, M. Bishop, Dennis B. Bowen, and Q. Qiu. Automatic image labeling with click supervision on aerial images. *2020 International Joint Conference on Neural Networks (IJCNN)*, pages 1–8, 2020.
- [39] Sumit Bam Shrestha and Garrick Orchard. Slayer: Spike layer error reassignment in time. In *Advances in Neural Information Processing Systems*, pages 1412–1421, 2018.
- [40] Chaklam Silpasuwanchai and Xiangshi Ren. Jump and shoot! prioritizing primary and alternative body gestures for intense gameplay. In *Proceedings of the SIGCHI Conference on Human Factors in Computing Systems*, CHI '14, page 951–954, New York, NY, USA, 2014. Association for Computing Machinery.
- [41] K. Stewart, G. Orchard, S. B. Shrestha, and E. Neftci. Online few-shot gesture learning on a neuromorphic processor. *IEEE Journal on Emerging and Selected Topics in Circuits and Systems*, 10(4):512–521, 2020.
- [42] K. Stewart, G. Orchard, S. B. Shrestha, and E. Neftci. Online few-shot gesture learning on a neuromorphic processor. *IEEE Journal on Emerging and Selected Topics in Circuits and Systems*, 10(4):512–521, Oct 2020.
- [43] Theophanis Tsandilas. Fallacies of agreement: A critical review of consensus assessment methods for gesture elicitation. *ACM Trans. Comput.-Hum. Interact.*, 25(3), June 2018.
- [44] Radu-Daniel Vatavu. User-defined gestures for free-hand tv control. In *Proceedings of the 10th European Conference on Interactive TV and Video*, EuroITV '12, page 45–48, New York, NY, USA, 2012. Association for Computing Machinery.
- [45] Radu-Daniel Vatavu. The dissimilarity-consensus approach to agreement analysis in gesture elicitation studies. In *Proceedings of the 2019 CHI Conference on Human Factors in Computing Systems*, CHI '19, page 1–13, New York, NY, USA, 2019. Association for Computing Machinery.
- [46] Radu-Daniel Vatavu and Jacob O. Wobbrock. Formalizing agreement analysis for elicitation studies: New measures, significance test, and toolkit. In *Proceedings of the 33rd Annual ACM Conference on Human Factors in Computing Systems*, CHI '15, page 1325–1334, New York, NY, USA, 2015. Association for Computing Machinery.
- [47] Santiago Villarreal-Narvaez, Jean Vanderdonckt, Radu-Daniel Vatavu, and Jacob O. Wobbrock. A systematic review of gesture elicitation studies: What can we learn from 216 studies? In *Proceedings of the 2020 ACM Designing Interactive Systems Conference*, DIS '20, page 855–872, New York, NY, USA, 2020. Association for Computing Machinery.
- [48] Saiwen Wang, Jie Song, Jaime Lien, Ivan Poupyrev, and Omar Hilliges. Interacting with soli: Exploring fine-grained dynamic gesture recognition in the radio-frequency spectrum. In *Proceedings of the 29th Annual Symposium on User Interface Software and Technology*, UIST '16, page 851–860, New York, NY, USA, 2016. Association for Computing Machinery.
- [49] Laurenz Wiskott and Terrence J Sejnowski. Slow feature analysis: Unsupervised learning of invariances. *Neural computation*, 14(4):715–770, 2002.
- [50] Jacob O. Wobbrock, Meredith Ringel Morris, and Andrew D. Wilson. User-defined gestures for surface computing. In *Proceedings of the SIGCHI Conference on Human Factors in Computing Systems*, CHI '09, page 1083–1092, New York, NY, USA, 2009. Association for Computing Machinery.
- [51] Gareth Young, Hamish Milne, Daniel Griffiths, Elliot Padfield, Robert Blenkinsopp, and Orestis Georgiou. Designing mid-air haptic gesture controlled user interfaces for cars. *Proceedings of the ACM on Human-Computer Interaction*, 4(EICS):1–23, Jun 2020.
- [52] Friedemann Zenke and Surya Ganguli. Superspike: Supervised learning in multi-layer spiking neural networks. *arXiv preprint arXiv:1705.11146*, 2017.
- [53] F. Zenke and E. O. Neftci. Brain-inspired learning on neuromorphic substrates. *Proceedings of the IEEE*, pages 1–16, 2021.
- [54] Z. Zhang. Microsoft kinect sensor and its effect. *IEEE MultiMedia*, 19(2):4–10, 2012.